

# Object Detection Using Hausdorff Distance and Multiclass Discriminative Field

Xiaofeng Zhang<sup>1</sup>, Hong Ding<sup>1</sup> and Rengui Cheng<sup>2</sup>

<sup>1</sup>*School of Computer Science and Technology, Nantong University, Nantong, China*

<sup>2</sup>*Department of Mathematics and Computer Science,  
Wuyi University, Nanping, China  
ntuzxf@163.com*

## Abstract

*In this paper, we present a novel object detection scheme using only local contour fragments. A sample fragment extraction method decomposes a whole contour into several parts. Then, the candidate locations of corresponding fragments in test images are detected by a modified Hausdorff distance with punishment on clutter edge regions. The most probable locations are selected by Multiclass Discriminative Field (MDF). Finally, contours of the objects can be drawn with these locations and sample fragments. Our major contributions are simplifying the MDF by an undirected graph constructed by the candidate locations and directly selecting the fragment locations by this MDF. The results on our postmark database and the ETHZ database from internet show that the proposed scheme is practicable.*

**Keywords:** *object detection, fragment extraction, Hausdorff distance, Multiclass Discriminative Field*

## 1. Introduction

Object detection, which is used to separate interested objects from backgrounds, acts as a critical role in image retrieval, scene understanding and so on. In the past few years, it has received a lot of attentions. Many features, which play an important role in object detection, are proposed for object detection. In addition to the features using region or point character [1-3], recently several approaches based on contour features have been proposed [4-6].

In some cases, objects may be recognized by their colors or textures. But in most cases it is not true. Figure 1 shows some examples of apple logo. They belong to the same category while having different colors and textures. People can easily recognize these apple logos by their shapes, which demonstrates that the contour can be used as an important clue in object detection. In this case, contour feature has many advantages over texture, such as it is adapt to lighting or color variation. It is with this reason that several approaches choose contour information to explore object recognition systems [4-6]. Most of these approaches select the center of objects by Hough voting. After obtaining the center of the object, they have to apply post operations to get the contours of objects. In this work, we will directly select the fragment locations by Multiclass Discriminative Field (MDF).

When using contour features, a contour is usually decomposed into several fragments. There are many local fragment detectors such as shape context [7-8], shapeme [9] and pAS [10]. Shape context, which is a good local descriptor, can represent the similarity of pixels and their surrounding. It is time-consuming and usually suitable to small objects. Shapeme, which uses Geometric Blur operator to describe local shape, can distinguish foreground from

background. pAS is a kind of kAS which has k connected or nearby parts and pAS is the best one among the kAS. It also can well describe the local features.



**Figure 1. Apple Logos with Different Colors and Textures**

We propose an approach which detects corresponding contours from a test image in the following scheme. First, the sample contour is obtained by the Canny edge detector from a sample image and decomposed into several sample fragments. The test image is converted to an edge distance image. Then each fragment's candidate locations are detected by a modified Hausdorff distance. Finally, the locations confirmed from the candidates by MDF are connected into the contours.

The overall structure of the paper is as follows. Section 2 describes sample fragment extraction from sample image and corresponding fragment detection in a test image. Section 3 gives how to select the locations of fragments by MDF. The technique is evaluated in Section 4, and conclusions are given in Section 5.

## 2. Local Fragment Detection

In this section we decompose the sample contour into several sample fragments and detect corresponding fragments in a test image by a modified Hausdorff distance with punishment on clutter edge regions.

### 2.1. Sample Fragment Extraction

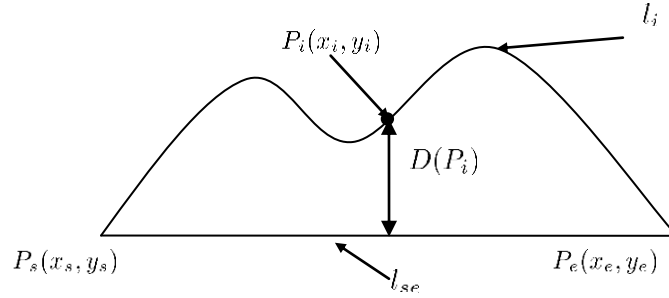
We decompose a contour into several fragments for better adapting to the deformation conditions. In order to get fragments with enough discriminative information, our sample fragments should have following features.

1.  $L_{l_i \in N}(l_i) > L_t$ , where  $L(l_i)$  is the length of sample fragment  $l_i$ ,  $N$  is the set of sample fragments and  $L_t$  is the length threshold. This criterion ensures a local fragment is long enough.

2.  $\max_{P_i \in N_j}(D(P_i)) > D_t$ , where  $N_j$  is the point set of the local fragment  $j$ ,  $D(P_i)$  is the distance of a point  $P_i(x_i, y_i)$  to  $l_{se}$ ,  $P_i(x_i, y_i)$  is a point of the sample fragment and  $l_{se}$  is the line between start point  $P_s(x_s, y_s)$  and end point  $P_e(x_e, y_e)$  and  $D_t$  is a distance threshold. This criterion ensures the sample fragments are not slim as a line. The distance  $D(P_i)$  can be calculated by

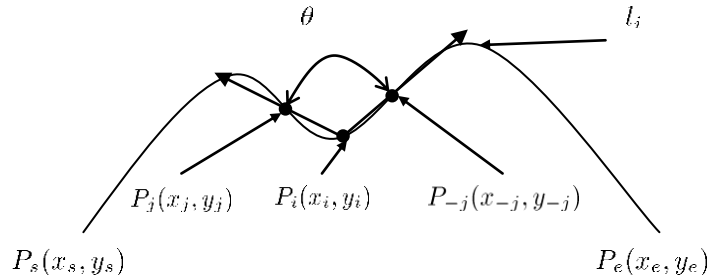
$$D(P_i) = \frac{|(y_e - y_s)(x_i - x_s) - (x_e - x_s)(y_i - y_s)|}{\sqrt{(y_e - y_s)^2 + (x_e - x_s)^2}}. \quad (1)$$

Figure 2 illustrates the relation between  $P_i(x_i, y_i)$ ,  $P_s(x_s, y_s)$ ,  $P_e(x_e, y_e)$  and  $D(P_i)$ .



**Figure 2. Distance from the Edge Point  $P_i(x_i, y_i)$  to the Line  $l_{se}$**

3. Neither start point  $P_s$  nor end point  $P_e$  should be a salient. As illustrate in Figure 3, a contour point  $P_i(x_i, y_i)$  has angle  $\theta$  ( $\theta \in [0, \pi)$ ). Two rags  $P_iP_j$  and  $P_iP_{-j}$  proceeding from  $P_i$  form the angle  $\theta$ , where  $P_j(x_j, y_j)$  and  $P_{-j}(x_{-j}, y_{-j})$  are two contour points with same distance to  $P_i(x_i, y_i)$  but in different directions. The smaller  $\theta$  is, the more salient  $P_i$  should be. So, the  $\theta$  of  $P_s$  and  $P_e$  should larger than  $\theta_t$  ( $\theta_t$  is a threshold). This criterion can avoid some improper decomposition.



**Figure 3. A Point  $P_i(x_i, y_i)$  with Angle  $\theta$ .  $P_i(x_i, y_i)$  is a Point of the Contour,  $P_j(x_j, y_j)$  and  $P_{-j}(x_{-j}, y_{-j})$  are Two Points of the Contour with Same Distance to  $P_i(x_i, y_i)$  but in Different Directions**

With these criterions, the local fragments can be extracted automatically. Firstly, select a contour point never being visited and use it as the start point of a curve. Secondly, the curve grows until its length over a threshold  $L_t$ . Thirdly, check  $D(P_i)$  of every point. If  $\max_{P_i \in N_j} D(P_i)$  is less than a threshold  $D_t$ , grow the curve until this criterion is satisfied. Fourthly, check whether start point  $P_s$  and end point  $P_e$  are salient points. The curve should grow until neither of them is a salient point. A curve which satisfies all these criterions is a fragment. The fragments of apple logo are shown in Figure 4 ( $L_t = 30$ ,  $D_t = 3$  and  $\theta_t = \pi/2$ ).

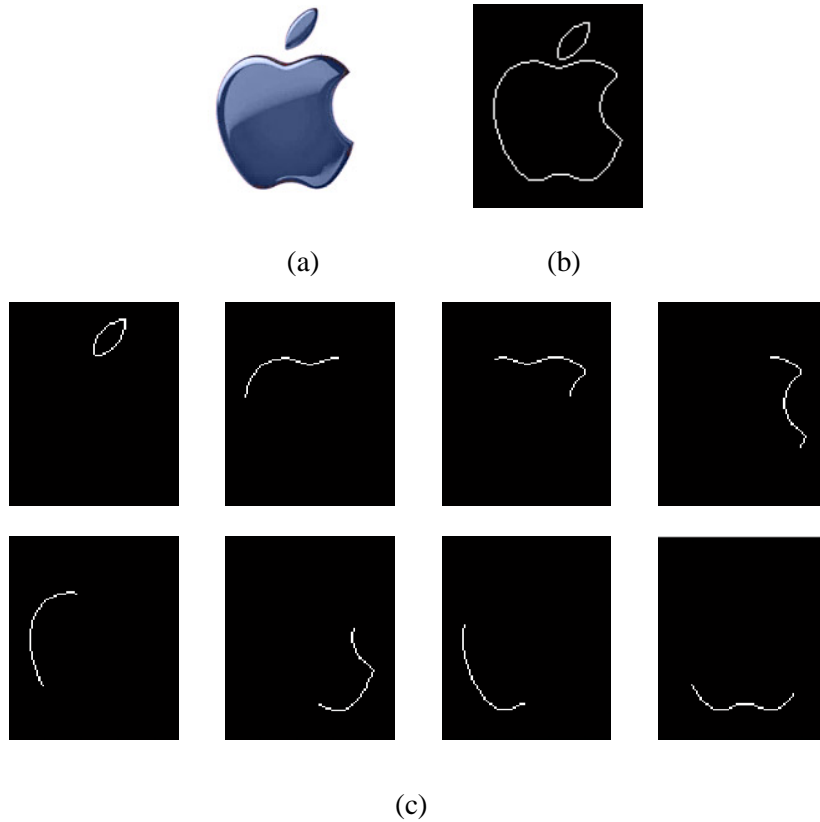


**Figure 4. Sample Fragments of Apple Logo: (a) Sample Image, (b) Contour of (a), (c) Sample Fragments of (b)**

## 2.2. Candidate Location Detection

In order to detect candidate locations of fragments in test images, we use a modified Hausdorff distance.

Hausdorff distance, which is a method of comparing two sets, can be used to determine the degree of resemblance between two objects. Given two finite sets of points  $A = \{a_1, a_2, \dots, a_n\}$  and  $B = \{b_1, b_2, \dots, b_n\}$ , the Hausdorff distance is defined as [11]

$$H(A, B) = \max(h(A, B), h(B, A)), \quad (2)$$

where  $h(A, B) = \max_{a \in A} \min_{b \in B} \|a - b\|$  and  $h(B, A) = \max_{b \in B} \min_{a \in A} \|b - a\|$ .  $\|\cdot\|$  is some underlying norm on the sets  $A$  and  $B$ , here, we use Euclidean norm. In most cases,  $h(A, B) \neq h(B, A)$ .

To detect whether the edges  $B$  of a test image contains a fragment  $A$ , the partial Hausdorff distance can be used, that is

$$H(A, B) = h(A, B). \quad (3)$$

Next we use Hausdorff distance denotes partial Hausdorff distance. The partial Hausdorff distance can be efficiently calculated by edge distance image whose values of edge points are zero and values of other points increase as their distance from edge points increasing.

When the objects have fake edges or are partly occluded, Hausdorff distance can hardly get the accurate result. If only few fragments are not detected, the contour can still be detected according to the rest fragments. So, the partly occlusion can be solved by decomposing a sample contour into fragments.

It is well know that an average operation is more insensitive to fake edges than a maximum operation, so it is reasonable to replace the maximum operation in  $h(A, B)$  with an average operation. Then, the partial Hausdorff distance can be rewrite as

$$h(A, B) = \frac{1}{N_a} \sum_{a \in A} d(a, B), \quad (4)$$

where  $d(a, B) = \min_{b \in B} \|a - b\|$ ,  $N_a$  is the number of points in fragment  $A$ .

In order to further improve Hausdorff distance performance, Takacs proposed a modified Haudorff distance with punishment and their  $d(a, B)$  was [12]

$$d(a, B) = \max(I \min_{b \in N_B^a} \|a - b\|, (1 - I)F) \quad (5)$$

where  $N_B^a$  is the neighborhood of the point  $a$  in  $B$ ,  $F$  is a punishment and

$$I = \begin{cases} 1 & \text{if there exist a point } b \in N_B^a \\ 0 & \text{otherwise} \end{cases} \quad (6)$$

Their method only punishes the points without corresponding points in another set. However it is no use to cluttered edges. It seems that a punishment should also be applied to those points with too many corresponding points. Consider a punishment on clutter edges,  $I$  can be rewritten as

$$I = \begin{cases} 1 & \text{if } n_b = 1 \\ 0 & \text{otherwise} \end{cases} \quad (7)$$

Here,  $n_b$  is the number of fragments in  $N_B^a$ . As shows in Figure 5,  $N_B^a$  is the region in the circle, (a) has one fragment in  $N_B^a$  while (b) has two fragments in  $N_B^a$ . So the center point of Figure(b) should add a punishment while (a) does not need a punishment.

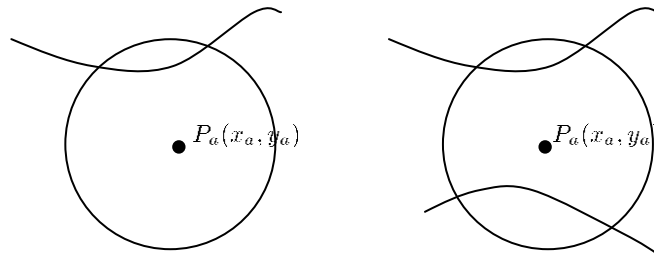


**Figure 5. Neighborhood of the Point  $P_a(x_a, y_a)$ .  $P_a$  is a Point of Sample Fragment  $A$ , the Region in the Circle is the Neighborhood of  $P_a$  and the Curves are Edges of a Test Image**

When  $I = 0$ , the punishment is applied in the edge distance image by setting the values of these points with an large value. Figure 6 shows an example of a punishment, (b) is the edge distance image of (a), (c) is the illustration of the punishment added to (b). In Figure 6(b) and (c), bright regions have large distance from edges and vice versa. (d) are two sample fragments, (e) and (f) show their corresponding locations in (b) and (c). Though the

punishment does not influence the results of first sample fragment, it significantly reduces the candidate locations of the second sample fragments which make the results more reasonable.

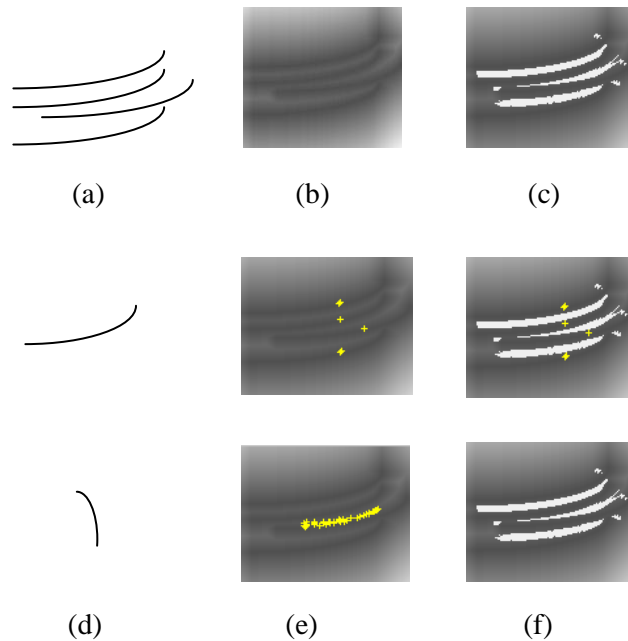


**Figure 6. A Sample of Adding Punishment in an Edge Distance Image. (a) Edges of a Test Image, (b) Edge Distance Image of (a), (c) Edge Distance Image with the Punishment on (b), (d) Two Sample Fragments, (e) and (f) Their Corresponding Locations in (b) and (c). Yellow Crosses are Center Points of Corresponding Fragments.**

Figure 7 shows the candidate locations detected by the modified Hausdorff method, the yellow cross labels are centers of each fragment. The crowded labels mean that in a local region there is more than one local maximum value.



**Figure 7. Locations Detected by Modified Hausdorff Method**

### **3. Fragment Selection by MDF**

In this section we describe a MDF method, which is a crucial step in our method. By this MDF, we can get the proper fragments of an object.

### 3.1. MDF Introduction

Condition Random Field (CRF) is one of Markov random field (MRF). It directly models the posterior distribution  $P(x|y)$  as a Gibbs field and conquers label bias of Hidden Markov Model (HMM). Kumar et al. developed the CRF to Discriminative Random Field (DRF) which is applied in image processing [13]. Then, they extended DRF to MDF which can handle multiclass labeling problems [14]. MDF obeys the distribution of DRF. In MDF, the distribution over all the labels  $x$  given the observations  $y$  can be written as

$$P(x|y) = \frac{1}{Z} \exp \left( \sum_{i \in S} A(x_i, y) + \sum_{i \in S} \sum_{j \in N_i} I(x_i, x_j, y) \right), \quad (8)$$

where  $Z$  is a normalizing constant known as the partition function,  $S$  is the set of all nodes,  $N_i$  is node  $i$ 's neighbourhood,  $A$  and  $I$ , which called as association potential and interaction potential, are the unary and pairwise potentials, respectively.

The association potential is

$$A(x_i, y) = \sum_{k=1}^C \delta(x_i = k) \log P'(x_i = k|y), \quad (9)$$

where  $C$  is the number of classes,  $\delta(x_i = k)$  is 1 if  $x_i = k$  and 0 otherwise,  $P'(x_i = k|y)$  is the probability of  $x_i$  belonging to class  $k$  under the observation  $y$ .  $\log$  operator ensures that the DRF is equivalent to a logistic classifier if the interaction potential is set to zero. The association potential is seen as a local decision term which decides the association of a given node to a certain class ignoring its neighbors.

The interaction potential is

$$I(x_i, x_j, y) = \sum_{k=1}^C \sum_{l=1}^C \nu_{kl}^T \mu_{ij}(y) \delta(x_i = k) \delta(x_j = l), \quad (10)$$

where  $\nu_{kl}^T$  are the model parameters and  $\mu_{ij}(y)$  encodes the pairwise features.  $\delta(\cdot)$  is the same as in (9). The interaction potential is seen as a data dependent smoothing function.

They construct an undirected graph for MDF. The nodes of the undirected graph are candidate patches of the object. due to every node of the graph, at the beginning of the method, is uncertain belonging to which category, MDF is a time-consuming algorithm, especially its training period [15].

### 3.2. Parameter Estimation

At this stage we generate an undirected graph for MDF. Every node  $x_i$  of the graph is a candidate location detected by the modified Hausdorff distance. A node  $x_i$  contains the information of its location and Hausdorff distance.

Smaller the Hausdorff distance is, higher probability the fragment belongs to the contour of an object. If a Hausdorff distance is less than a threshold only means that the location has a match of a fragment, the probability  $P'(x_i = k|y)$  can be set with a given initial value. Otherwise, we hope when Hausdorff distance is small, the probability decreases slowly with Hausdorff distance increasing, vice versa. Delta function is a nonlinear function which can describe this demand well. So, we can approximate the  $P'(x_i = k|y)$  by delta function [16]

$$P'(x_i = k|y) = \begin{cases} \frac{1}{2}(1 + \cos \frac{\pi H}{T_1}) & \text{if } H \leq T_1, \\ 0 & \text{otherwise} \end{cases}, \quad (11)$$

where  $H$  is a Hausdorff distance,  $T_1$  is a threshold.

$\nu_{kl}^T$  are the parameters between two categories (each category is a kind of fragment),  $k$  and  $l$ . In most cases, every fragment of an object only has one correct location, so we can set  $\nu_{kl}^T = 0$  if  $k = l$ . That means interaction potentials only relate the different category nodes and ignore the nodes in the same category.  $\mu_{ij}(y)$  is a pairwise feature, which indicates the similarity of the two neighbor nodes. So

$$\nu_{kl}^T \mu_{ij}(y) = f(D_{ij} - D_{kl}) \quad (12)$$

where  $f(\cdot)$  is a function,  $D_{ij}$  is the distance between two nodes  $i$  and  $j$ ,  $D_{kl}$  is the distance between two categories  $k$  and  $l$ , and  $i$  belongs to category  $k$ ,  $j$  belongs to category  $l$ . If a  $\nu_{kl}^T \mu_{ij}(y)$  less than a threshold only means that two nodes  $i$  and  $j$  belong to the same object, it can be set with a given initial value. Otherwise, it can also be set by the delta function

$$\nu_{kl}^T \mu_{ij}(y) = \begin{cases} \frac{1}{2}(1 + \cos \frac{\pi |D_{ij} - D_{kl}|}{T_2}) & \text{if } |D_{ij} - D_{kl}| \leq T_2, \\ 0 & \text{otherwise} \end{cases}, \quad (13)$$

where  $\mathcal{D}$  is Euclidean distance,  $T_2$  is a threshold. From (13), we know the node only relates with those nearby nodes in different categories.

So with the candidate fragments, we can get the model parameters. As illustrates in Figure 8, the yellow crosses are the center locations of fragments obtained by Hausdorff distance and the yellow lines means the two linked nodes have a relation.

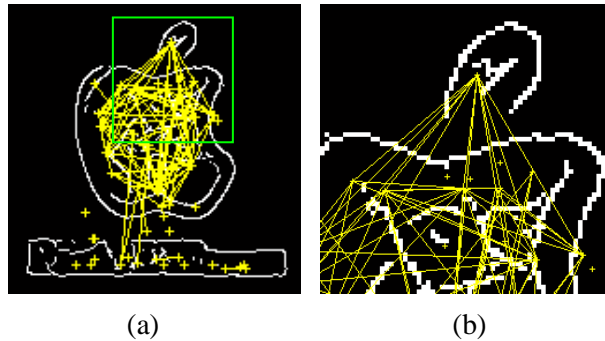


Figure 8. An Undirected Graph for MDF. (b) A part of (a).

### 3.3. Model Inference

With MDF model, we can calculate the posterior marginal of node  $x_i$  with label  $c_i$ . Loopy belief propagation (LBP) is used to infer the marginal estimates and it is a message passing algorithm proposed by Pearl [17].



With LBP, we get the message that node  $x_j$  pass to its neighbor  $x_i$  at iteration  $t$  [15]

$$m_{ji}^t(x_i) \leftarrow \alpha \sum_{x_j} \phi_j(x_j) \psi_{ij}(x_i, x_j) \prod_{k \in N_j \setminus i} m_{kj}^{t-1}(x_j) \quad (14)$$

where  $\alpha$  is the normalizer,  $\phi_j(x_j) = \exp(A(x_j|y))$ ,  $\psi_{ij}(x_i, x_j) = \exp(I(x_i, x_j, y))$ , and  $\setminus$  is set exclusion operator. The beliefs after  $t$  iterations are calculated as

$$b^t(x_i) = \kappa \phi_i(x_i) \prod_{j \in N_i} m_{ji}^t(x_i) \quad (15)$$

where  $\kappa$  is a normalized factor. We suppose that every fragment of an object only has one correct location, so we can rewrite  $m_{ji}^t(x_i)$  and  $b^t(x_i)$  as

$$m_{ji}^t(x_i) \leftarrow \alpha \sum_{x_j} \phi_j(x_j) \psi_{ij}(x_i, x_j) \prod_{k \in N_j \setminus i} \max_{l \in c_i} m_{kj}^{t-1}(x_j = l) \quad (16)$$

$$b^t(x_i) = \kappa \phi_i(x_i) \prod_{j \in N_i} \max_{l \in c_i} m_{ji}^t(x_i = l) \quad (17)$$

The graph generated in 3.2 can be inferred by LBP. The nodes with large value over a threshold will have high probability to be a correct fragment location. Figure 9(a) shows the results selected by MDF, the yellow cross labels are centers of fragments.

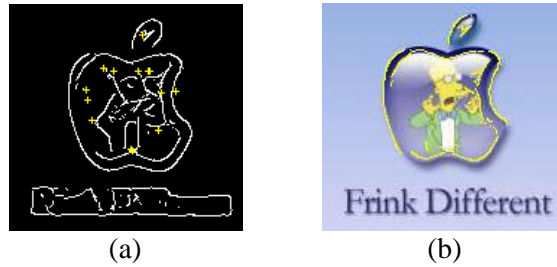


**Figure 9. Fragments Selected by MDF. (a) The Yellow Crosses are Centers of Fragments, (b) An Apple Logo Contour by Connecting the Fragments**

After getting the properly locations of every local fragment, contour can be drawn. We use the sample fragments as the templates and consider the edges corresponding to templates being the proper contour which is shown in Figure 9(b). Comparing with Hough voting, MDF has several advantages. First, MDF can directly select the fragments of the contour while Haugh voting selects the center of the object. Second, MDF can give the degree of similarity between the sample contour and the detected contour. If using the same parameters, we can find which one is more similar to the sample contour. For example, in Figure 10, the similarity between Figure 4(b) and Figure 10(a) is 98.93%, while the similarity between Figure 4(b) and Figure 10(b) is 91.38%. It is same with our sense that Figure 10(a) is more similar to the apple logo sample contour. Third, MDF can detect the deformation of the contour and can draw a relative closed contour. Comparing locations of the selected fragment and sample fragments, the degree of object deformation can be obtained. So we can slightly deform the fragment to adapt the deformation of object.



**Figure 10. The Similarity of (a) and (b) to Apple Sample in Figure 1(b) is 98.93% and 91.38%, respectively**

#### 4. Experiments

To evaluate the valid of the proposed method, we apply it to detect postmark on our envelop image database. The database has three groups and each group has 40 images. They are divided by their background complexities. As illustrates in Figure 11, these three columns belong to different groups. The postmarks in the first two groups have similar size and clear contours, while the postmarks in the last group have comparatively various size and blurred contours. The sample is selected randomly from the group with blank background. As discussed in Section 2, the sample contour is decomposed into  $n$  fragments, where  $n \in [6, 10]$  for both flexibility and simplicity. Then the candidates corresponding to sample fragments are detected from an edge distance image. These candidates form an undirected graph and the final fragments are selected by MDF. Some results with complex background are shown in Figure 12. The yellow marks are the contours of postmarks. All postmarks of the first two groups are detected without false-positive, while the performance of the last group is rather low. The statistical results of the last group are shown in Figure 13, where detection rate is the rate of postmark detection of all images in a group and false-positive per image is the average number of false-positive over all images in a group. The low performance of complex background is due to two reasons. One is the edges of postmarks are too blurred to detect and another is there are other parts more like a whole circle than these postmarks. Figure 14 shows some incorrect results, the contours of these postmark are not completely detected while there are other edges like a circle shape. So the method mistakes other edges for contour of a postmark.



**Figure 11. Postmarks and their Edges Detected by Canny Detector**

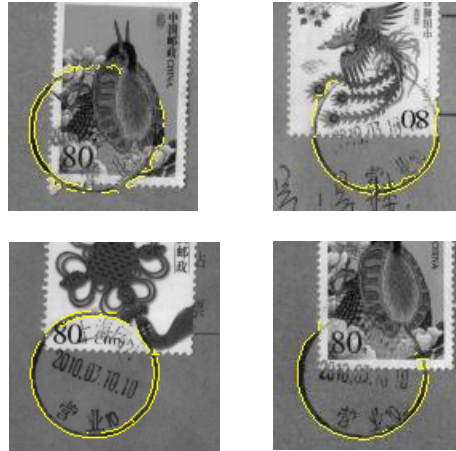


Figure 12. Some Results of Postmark Detection

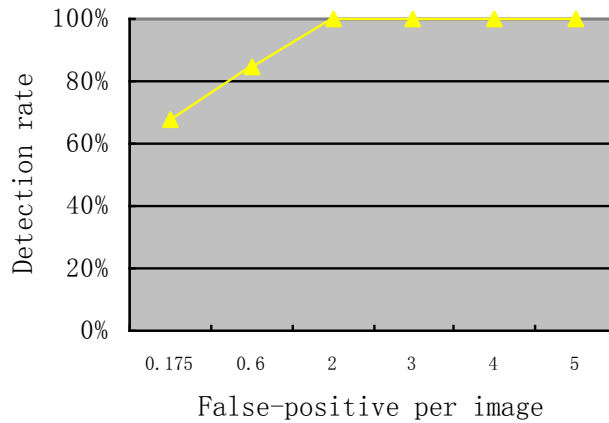


Figure 13. Postmark Detection Performance

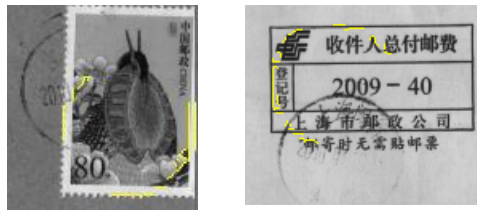


Figure 14. Some Incorrect Detection Results

We also applied our method on ETHZ shape classes [18] and selected a subset of this database to illustrate the results. Figure 15 shows some results of apple logo, giraffe and bottle. The first column is the sample contours which provided by ETHZ database and the rest are the results of test images. The first row are apple logo results, the sample is a contour with size  $93 \times 114$  and the rest are results of test images with sizes  $106 \times 154$ ,  $118 \times 136$ ,  $86 \times 108$  and  $114 \times 90$ , respectively. The next two rows have similar

conditions. It is obvious that with contour decomposition and MDF our method can tolerate some rotations and scale changes. The low performance on giraffes is mainly due to their large deformation.



**Figure 15. Some Results on ETHZ Database. The First Column is the Sample Contours and the Rest are the Detection Results**

## 5. Conclusion

In this paper, a method of object detection is proposed and the experiments show it is a practicable scheme. A sample contour is decomposed into several sample fragments. Then, candidate fragments corresponding to sample fragments are detected by a modified Hausdorff distance in test images. Using the undirected graph constructed by these candidates, MDF is simplified and used to select fragments. These fragments are connected to form the contour of the object. Only one sample is required and our model is tolerant to distortion, partly missing and various backgrounds. We have made contributions with our candidate fragment detection which makes MDF model simple. With this MDF, proper locations of fragments can be selected and final contours are drawn by connecting them directly.

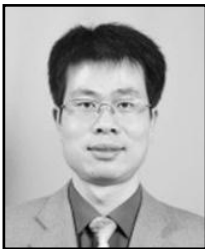
## Acknowledgements

This work is partially supported by the Education Department plan of Fujian Province (JA12321).

## References

- [1] S. Agarwal, A. Awan and D. Roth, "Learning to detect objects in images via a sparse, part-based representation", *IEEE Transactions on Pattern Analysis and Machine Intelligence*, vol. 26, no. 11, (2004), pp. 1475-1490.
- [2] E. Borenstein and S. Ullman, "Class-specific, top-down segmentation", *European conference on computer vision*, vol. 2351, (2002), pp. 109-122.
- [3] D. G. Lowe, "Distinctive image features from scale-invariant keypoints", *International Journal of Computer Vision*, vol. 60, no. 2, (2004), pp. 91-110.
- [4] J. Shotton, A. Blake and R. Cipolla, "Contour-based learning for object detection", *IEEE International Conference on Computer Vision*, (2005), pp. 503-510.
- [5] V. Ferrari, F. Jurie and C. Schmid, "From images to shape models for object detection", *International Journal of Computer Vision*, vol. 87, no. 3, (2010), pp. 284-303.
- [6] A. Opelt, A. Pinz and A. Zisserman, "A boundary-fragment-model for object detection", *European conference on computer vision*, (2006), pp. 575-588.
- [7] S. Belongie, J. Malik and J. Puzicha, "Shape matching and object recognition using shape contexts", *IEEE Transactions on Pattern Analysis and Machine Intelligence*, vol. 24, no. 4, (2002), pp. 509-522.
- [8] H. J. Seo and P. Milanfar, "Training-Free, Generic Object Detection Using Locally Adaptive Regression Kernels", *IEEE Transactions on Pattern Analysis and Machine Intelligence*, vol. 32, no. 9, (2010), pp. 1688-1704.
- [9] X. F. Ren, C. C. Fowlkes and J. Malik, "Figure/ground assignment in natural images", *European Conference on Computer Vision*, vol. 3952, (2006), pp. 614-627.
- [10] V. Ferrari, L. Fevrier, F. Jurie, *et al.*, "Groups of adjacent contour segments for object detection", *IEEE Transactions on Pattern Analysis and Machine Intelligence*, vol. 30, (2008), pp. 36-51.
- [11] D. P. Huttenlocher, G. A. Klanderman and W. J. Rucklidge, "Comparing Images Using The Hausdorff Distance", *IEEE Transactions on Pattern Analysis and Machine Intelligence*, vol. 15, no. 9, (1993), pp. 850-863.
- [12] B. Takacs, "Comparing face images using the modified Hausdorff distance", *Pattern Recognition*, vol. 31, no. 12, (1998), pp. 1873-1881.
- [13] S. Kumar and M. Hebert, "Discriminative fields for modeling spatial dependencies in natural images", *Advances in neural information processing systems*, vol. 16, (2004), pp. 1531-1538.
- [14] S. Kumar and M. Hebert, "Multiclass discriminative fields for parts-based object detection", *Snowbird Learning Workshop*, vol. 164, (2004).
- [15] S. Kumar, "Models for learning spatial interactions in natural images for context-based classification", PhD thesis, Citeseer, (2005).
- [16] H. K. Zhao, T. Chan, B. Merriman, *et al.*, "A variational level set approach to multiphase motion", *Journal of computational physics*, vol. 127, no. 1, (1996), pp. 179-195.
- [17] J. Pearl, "Probabilistic reasoning in intelligent systems: networks of plausible inference", Morgan Kaufmann, (1988).
- [18] V. Ferrari, T. Tuytelaars and L. Van Gool, "Object detection by contour segment networks", *European conference on computer vision*, vol. 3953, (2006), pp. 14-28.

## Authors



**Xiaofeng Zhang** received the B.S. degree in computer science from Soochow University, China, in 2002, the M.S. degree from Shanghai Normal University, China, in 2009. He is a lecturer of School of Computer Science and Technology, Nantong University, China. His research interests focus on computer vision and its applications.



**Hong Ding** received the B.S. degree and the M.S. degree in computer science from Soochow University, China, in 2002 and 2005, respectively. She is a lecturer of School of Computer Science and Technology, Nantong University, China. Her research interests include image recognition and retrieval, medical image processing.



**Rengui Cheng** received the B.S. degree in physics education from Fujian Normal University, China, in 1994, the M.S. degree in computer science from Northwest University, China, in 2001. He is an associate professor of Department of Mathematics and Computer Science, Wuyi University, China. His research interests include compute vision, digital image processing and pattern recognition.